Applied Mathematical Modelling 66 (2019) 332–343

Contents lists available at ScienceDirect

Applied Mathematical Modelling

journal homepage: www.elsevier.com/locate/apm

Deflagration-to-detonation transition in pipes: The analytical theory

Boo-Hyoung Bang[a,b], Chan-Sol Ahn[a,c], Young-Tae Kim[b], Myung-Ho Lee[b], Min-Woo Kim[a], Alexander L. Yarin[d,*], Sam S. Yoon[a,*]

[a] School of Mechanical Engineering, Korea University, Seoul 136-713, South Korea
[b] Technology Development Team, Daewoo Institute of Construction Technology, 60, Songjuk-dong, Jangan-gu, Suwon 440-210, South Korea
[c] Fire Research Center, Korea Institute of Construction Technology, 283, Goyang-daero, Ilsanseo-gu, Goyang-si 10223, South Korea
[d] Department of Mechanical & Industrial Engineering, University of Illinois at Chicago, 842 W. Taylor St., Chicago 60607, USA

ARTICLE INFO

Article history:
Received 5 February 2018
Revised 27 August 2018
Accepted 12 September 2018
Available online 21 September 2018

Keywords:
Deflagration
Detonation
Transition
Shock wave
Pressure rise

ABSTRACT

Herein, we discuss the fundamental aspects of the deflagration-to-detonation transition (DDT) phenomenon in the framework of the analytical theory. This semi-empirical approach facilitates prediction of the pressure rise and the shock wave speed for a given fuel type and concentration, which may be of significant interest for the design and assessment of petrochemical plants by field-safety engineers. The locally observed DDT phenomenon explored in the present experiments is also discussed, and the measured pressure rise is compared with the theoretical predictions.

1. Introduction

Deflagration-to-detonation transition (DDT) occurs under circumstances such as those in underground coal mine explosions and in accidents that accompany transmittance and storage involving pipe flows in petrochemical or liquefied natural gas plants. Though DDT accidents are infrequent, they are still very dangerous and generally lead to a catastrophic loss of life and property. Because DDT is accompanied by extremely high pressures, its aftermath leads to devastating structural damage. Therefore, it is essential to estimate the effect of DDT for quantitative risk analysis of petrochemical plants. Hydrogen accumulation due to unexpected leaks in nuclear power plants is also a potential route to a DDT accident.

The fundamentals of the theory of detonation were established in the classical works of Rankine, Hugoniot, Lord Rayleigh, Chapman, and Jouguet [1]. The seminal theoretical and experimental works of Landau, Zel' dovich, and Shchelkin laid the foundations of the modern analytical theory of DDT. The key physico-chemical and aerodynamic elements are described in the fundamental texts [2,3], whereas the comprehensive analytical theory of DDT is presented in a monograph [4]. Two comprehensive reviews of the Soviet and American research related to DDT were published in 1973 and 1984 in [5,6]. A review of experimental and numerical studies on detonation and DDT can be found in Ref. [7].

Laser systems were used as a light source for stroboscopic Schlieren imaging to capture the DDT phenomenon [8]. The shock fronts, flame, and the DDT images were captured, in turn leading to the explanation of DDT as a phenomenon

* Corresponding authors.
E-mail addresses: ayarin@uic.edu (A.L. Yarin), skyoon@korea.ac.kr (S.S. Yoon).

https://doi.org/10.1016/j.apm.2018.09.023
0307-904X/

associated with the transformation and instability of the turbulent flame front following the leading shock wave. The fuel concentration limits that sustain the detonation phenomenon were investigated [9], and the effect of the tube geometry on DDT was studied [5,10,11].

The classical explanations of DDT are centered on flame acceleration as the triggering mechanism. Two factors were proposed to be responsible for this acceleration: flame turbulization accompanied by significant growth of the flame area, and thus the rate of combustion [4] and Zeldovich's mechanism involving a gradient ahead of the flame front or at the flame front responsible for flame stretching [3,12]. Numerical two-dimensional (2D) solutions of the reactive Navier–Stokes equations for laminar flows in channels with obstacles at the walls revealed that diffracting shocks reflecting from the wall and colliding with an obstacle, or collision of the leading shock with the obstacles, create hot spots ahead of the flame, which produces detonation according to Zeldovich's gradient mechanism [13]. Numerical 2D and 3D simulations also reveal that the surface area of the flame increases due to shock-flame interactions, and the Rayleigh–Taylor, and Kelvin–Helmholtz instabilities, as well as flame-vortex interactions in the obstacle wakes, while the Richtmyer–Meshkov instability is triggered by shock-flame interactions [14].

These mechanisms of flame stretching are essentially complementary to Shchelkin's direct flame turbulization mechanism. More recent numerical simulations by the same group led by Oran [15,16] fully corroborate these findings, essentially providing a detailed account of flame-stretching mechanisms that result in DDT in channels with rough walls.

Enhanced dissipation near rough channel walls can increase the near-wall temperature, which results in flame stretching in a tulip-like form and near-wall thermal explosion, i.e. DDT [17–19]. Note that the near-wall dissipation initially leads to flame acceleration. Being ignited at the pipe axis, the flame initially takes a finger-like shape and accelerates because of the increase in the flame area. Then, such flame decelerates before tulip-like flame forms due to flame-wall interactions [20–22].

Recently [23], Kagan and Sivashinsky revealed that with a single reaction, the compression in the pre-heat zone ahead of the flame does not reach the ignition threshold, which invalidates Zeldovich's gradient mechanism of DDT in this case. As a possible remedy, formation of an expanding wrinkled flame is proposed, which could essentially be linked to Shchelkin's mechanism of DDT. As a supplementary mechanism triggering DDT, Sivashinsky and coworkers [24,25] discussed dissipation due to hydraulic resistance in the framework of a 1D model, where this dissipation results in additional pre-heating and pre-compression of the fuel-oxidizer mixture ahead of the flame, which in turn could cause thermal explosion, and thus DDT. This 1D mechanism of thermal gas explosion between the flame front and the leading shock wave is essentially similar to the 2D near-wall thermal explosion described in Refs. [17–19].

Liberman et al. [26] studied DDT based on experiments and numerical solutions of the 2D reactive Navier–Stokes equations for a hydrogen-oxygen mixture, accounting for the detailed chemical kinetics. Their experimental findings revealed that DDT begins as a localized thermal explosion of gas between the flame front and the leading shock wave. Their 3D numerical solution of the laminar flow problem showed that DDT can be caused by accelerated flame stretching along the channel walls, leading to steepening of the shock ahead of it and formation of a high-pressure pulse before the flame. That is, the DDT mechanism is postulated to involve positive feedback between the pressure rise and the chemical reaction ahead of the flame, resulting in thermal explosion under laminar flow conditions. The DDT mechanism under the conditions studied in Refs. [26,27] differs from Zeldovich's gradient mechanism of DDT. Despite the different conditions, the flame restructuring and acceleration are in agreement for both cases, as demonstrated by the experimental and numerical studies by the same group [28]. Liberman and coworkers [29,30] also showed that accounting for the detailed chemical kinetics increases the induction time of the pre-flame chemical reaction, in contrast with the predictions from a single Arrhenius reaction, which invalidates Zeldovich's gradient mechanism of DDT, as also illustrated in Ref. [23]. Under special conditions, when light-adsorbing particles are dispersed in a gaseous fuel-oxidizer mixture, radiation heat transfer from the flame zone creates the temperature gradient required for Zeldovich's gradient mechanism of DDT [31–33].

Poludnenko et al. [34] suggested a critical turbulent flame speed as a determining criterion for the onset of DDT. Kagan and Sivashinsky [35] numerically explored the effect of the boundary conditions on the DDT process in circular tubes. Ciccarelli and Dorofeev [36] also suggested a criterion for flame acceleration and DDT. They explored the effect of obstacles on flame acceleration. They also explained the effect of the mixture composition and the initial temperature and pressure on the critical expansion ratio between the unburned and burned gases and the formation of a supersonic combustion regime by introducing the flame thickness effect.

Theoretical and numerical predictions related to the effect of detonation-triggered explosion on pipeline bending were presented and the data were compared with the experimental data [37,38].

The experimental and numerical approaches considered above mostly deal with narrow pipes and laminar regimes. On the other hand, DDT in wide pipes with turbulent combustion and flow has rarely been addressed in these studies. Even though turbulence might not be required for DDT in narrow smooth pipes, for wide pipes with turbulent combustion, the associated Shchelkin's mechanism of DDT remains a viable and realistic option, and is essentially unaffected by the recent laminar modeling appropriate for narrow smooth pipes. In engineering practice, an immediate assessment of possible DDT in wide pipes with turbulent flow is highly desirable, which can be achieved in the framework of the theoretical approach discussed in the present study.

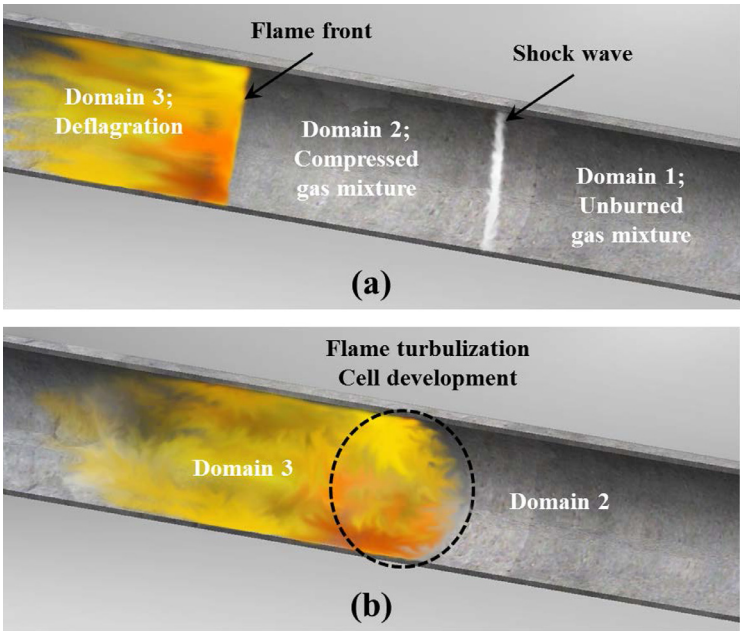

Fig. 1. (a) Gasdynamic pattern of the three domains characteristic of flame propagation in wide pipes according to Refs. [3,4]. (b) A non-gasdynamic element: flame turbulization that can trigger the deflagration-to-detonation transition (DDT) [4].

2. General physical aspects of DDT

A flame propagating in a wide pipe issues hot products of combustion. Thermal expansion of the latter causes the flame front to essentially act as a piston, which compresses the fresh fuel-oxidizer mixture ahead of the flame front. As a result, the propagating flame front, as a propagating piston, generates ahead compression waves. These waves move with the local speed of sound, i.e. faster than the flame front. Accordingly, the distance between the flame front and the first compression wave increases. Moreover, the compression waves that follow the preceding compression waves over the fresh mixture move faster, as the gas is already adiabatically compressed (and thus, heated) by the preceding waves. As a result, the following compression waves generated by the propagating flame reach the preceding ones, and thus, form a shock wave [4,39].

Accordingly, the pipe becomes subdivided into three domains (Fig. 1(a)): (1) the fresh fuel-oxidizer mixture ahead of the shock wave, (2) the compressed fuel-oxidizer mixture between the flame (the deflagration) front and the shock wave, and (3) the reaction products. Therefore, the flow pattern involves two discontinuity fronts: the shock wave, and the flame front (Fig. 1(a)). It should be emphasized that in the shock wave, the fresh mixture is compressed (i.e., the shock wave is a compression wave), and the compression is non-isentropic as it is accompanied by dissipation due to viscous losses. On the contrary, the deflagration wave (the flame front), is a rarefaction wave as the combustion products behind it expand due to heat released by the combustion reaction in the flame. Without this heat release, the existence of rarefaction waves is forbidden by the Zemplen theorem. However, with chemical heat release, rarefaction waves can occur, and the deflagration wave is a manifestation of this phenomenon. It should be emphasized that the flow pattern depicted in Fig. 1(a) can be treated in the framework of the 'gasdynamics' approach in the one-dimensional approximation, namely, using the Rankine–Hugoniot jump conditions [4,40], as described in Sections 2.1 and 2.2.

The DDT occurs when the deflagration front (Fig. 1(a)) begins to accelerate and approaches the shock wave (Fig. 1(a)) [3,4]. Thereafter, the shock wave with the adjacent deflagration front forms the detonation wave, which propagates with the velocity determined using the Jouguet condition, i.e., with the steady-state velocity corresponding to the tangency of the Rayleigh and Hugoniot lines. Herein, however, the focus is on the transient DDT rather than on the steady-state detonation.

The acceleration of the deflagration wave leading to DDT results from an increase in the flame front area, which effectively increases the overall rate of combustion; nevertheless, the combustion mechanism of the latter can stay the same or even incorporate additional kinetic paths triggered by higher temperatures, elevated by compression [3,4].

Accordingly, the normal speed of combustion determined by the Zel'dovich–Frank–Kamenetsky formula [3,39] can vary due to kinetics changes, but the deflagration mechanism stays essentially the same. However, the flame front area can dramatically increase due to (i) Landau–Darrieus instability [4, 41,42], an especially important factor in narrow pipes with relatively low Reynolds numbers, (ii) 'isothermal' flow turbulence (characteristic of flows in wide pipes with high Reynolds numbers) according to Shchelkin's mechanism of DDT [4], (iii) artificial flow turbulization (such as increasing wall roughness) [3,4], and (iv) the turbulence generated by the flame itself [4]. Due to all these factors acting in concert or separately, the flame front becomes undulating, as illustrated in Fig. 1(b). This factor can trigger flame acceleration under

the non-gasdynamic conditions discussed in Section 2.3. These conditions together with the gasdynamics represented by the equations in Section 2.1 lead to DDT according to Shchelkin's mechanism. It should be emphasized that 'gasdynamic', is a conventional term [1] that refers to the Rankine–Hugoniot approach involving jump conditions, whereas 'non-gasdynamic' refers to all the phenomena triggered by the dissipation effects and instabilities, which stem from the 'gasdynamic' skeleton, and go beyond. Note that these definitions and terminology are standard and common.

2.1. Gasdynamic pattern of flame propagation in pipe from a closed end or symmetrically from an ignition center inside the pipe

The gasdynamic pattern, which is founded on the basic gasdynamics principles, is discussed in full detail in Ref. [4]. Here, we summarize the main results relevant in the present context and explain how they are inter-related and follow one another. The more detailed derivations are available in Ref. [4]. A flame propagating in a pipe from a closed end leaves behind stagnant combustion products, corresponding to the absolute velocity of the gas in domain 3 (Fig. 1(a)), where $u_3^+ = 0$ (here and hereinafter, the notations of Ref. [4] are used). It should be emphasized that the gasdynamic approach adopted in the present and the following sections lumps all the parameters over domains $1-3$ (Fig. 1). Thus, the boundary condition at the closed pipe end requires u_3^+ to be zero over all of domain 3. The Rankine–Hugoniot jump conditions on the shock wave and flame fronts in Fig. 1(a), i.e., the jump conditions for the mass, momentum, and total energy, can then be rearranged into the form of Eq. (1).

The density of the compressed mixture behind the shock wave, ρ_2, follows the relation:

$$\sigma = \frac{\kappa + \mu}{\kappa\mu + 1} \tag{1}$$

where $\mu = p_2/p_1$ (with p_1 being a given pressure before the shock wave, and p_2 being the pressure of the compressed gas between the shock wave and the flame front; $\mu \geq 1$), $\sigma = \rho_1/\rho_2$ (with ρ_1 being a given mixture density before the shock wave, and ρ_2 being the density of the compressed mixture between the shock wave and the flame front; $\sigma \leq 1$); the dimensionless parameter $\kappa = (\gamma+1)/(\gamma-1)$, where $\gamma = c_p/c_v$ is the adiabatic index, i.e., the ratio of the specific heat at constant pressure to the specific heat at constant volume. It should be emphasized that the same value of γ is used for each domain represented in Fig. 1(a).

The absolute velocity of the compressed mixture behind the shock wave and before the flame front, w, follows the relation:

$$\frac{w}{c_1} = (\mu - 1)\sqrt{\frac{2}{\gamma[(\gamma-1) + \mu(\gamma+1)]}} \tag{2}$$

where c_1 is the speed of sound before the shock wave (a known parameter). It should be emphasized that here and hereinafter, the absolute velocity is reckoned relative to the tube wall.

The pressure behind the flame front (the deflagration wave), p_3, follows the relation:

$$\pi_3' = \frac{\mu\left[\kappa - \sigma_3'/\sigma + 2\gamma Q/\left(c_1^2\mu\sigma\right)\right]}{\left(\kappa\sigma_3'/\sigma\right) - 1} \tag{3}$$

where $\pi_3' = p_3/p_1$, with p_3 being the pressure in the combustion products behind the deflagration wave, $\sigma_3' = \rho_1/\rho_3$ with ρ_3 being the density of the combustion products behind the deflagration wave, and Q being the heat released in the flame front.

The flame velocity relative to the compressed mixture behind the shock wave, u_+' follows the relation:

$$\frac{u_+'}{c_1} = \sqrt{\frac{\left(\pi_3'/\mu - 1\right)}{\left(1 - \sigma_3'/\sigma\right)}\frac{\mu\sigma}{\gamma}} \tag{4}$$

It should be emphasized that in the gasdynamic approach adopted here, the flame (like a shock) is considered as a discontinuity. This approximation has been very fruitful in multiple problems related to combustion and DDT theory [3,4] due to the relatively low thickness of the laminar flame compared to the other sizes involved. In the case of turbulent combustion, the flame front becomes wider, but is still assumed to be much smaller than the pipe diameter and the lengths of domains $1-3$ (Fig. 1).

An additional relation for the density ratios involving the absolute flame velocity, U, is as follows:

$$\frac{\sigma}{\sigma_3'} = 1 - \frac{w}{U} \tag{5}$$

The expression for U resulting from the Rankine–Hugoniot conditions for the total energy is described by:

$$\frac{U^2}{\gamma - 1} + U\left[\frac{Q}{w} - w\left(\frac{\gamma}{\gamma-1} - \frac{3}{2}\right)\right] - \left(\frac{c_1^2}{\gamma-1}\mu\sigma + Q + \frac{w^2}{2}\right) = 0 \tag{6}$$

It should be emphasized that if the pressure jump at the shock wave $\mu = p_2/p_1$ is given (as it will be provided by the non-gasdynamic condition related to flame turbulization discussed in Section 2.3), then the value of $\sigma = \rho_1/\rho_2$ (i.e.,

essentially the density, ρ_2, of the mixture compressed by the shock wave and preceding the flame front) is found from Eq. (1). The absolute velocity of the compressed mixture, w, is then found from Eq. (2) and the absolute velocity of the deflagration wave (the flame front), U, is found from Eq. (6). Thereafter, the ratio $\sigma_3' = \rho_1/\rho_3$ (i.e., essentially the density ρ_3 of the combustion products) is found from Eq. (5) and the value of $\pi_3' = p_3/p_1$ (i.e., essentially the pressure p_3 of the combustion products) is found from Eq. (3). The flame velocity relative to the compressed mixture behind the shock wave u_+' is then found from Eq. (4).

2.2. Gasdynamic pattern of flame propagation in pipe from an open end

When the deflagration front propagates from an open end of a pipe, the pressure in the combustion products $p_3 = p_1$ (where p_1 is the pressure of the unperturbed mixture before the shock wave). Accordingly, $\pi_3' = 1$. For a given pressure jump at the shock wave $\mu = p_2/p_1$, the value of $\sigma = \rho_1/\rho_2$ (essentially the density ρ_2 of the mixture compressed by the shock wave and preceding the flame front) is found from Eq. (1). Thereafter, the absolute velocity of the compressed mixture w is found from Eq. (2). Using the fact that now $\pi_3' = 1$, Eq. (3) takes the following form:

$$1 = \frac{\mu\left[\kappa - \sigma_3'/\sigma + 2\gamma Q/\left(c_1^2\mu\sigma\right)\right]}{\left(\kappa\sigma_3'/\sigma\right) - 1} \tag{7}$$

The latter equation is used to find the ratio $\sigma_3' = \rho_1/\rho_3$, i.e., essentially the density ρ_3 of the combustion products. Note also that $U = u_+' + w$.

It should be emphasized that the pressure jump at the shock wave $\mu = p_2/p_1$ will be provided by the non-gasdynamic condition related to flame turbulization discussed in Section 2.3, which will also determine the condition under which the deflagration front propagating from the open end of the pipe would accelerate and transform into a detonation wave (DDT).

2.3. Flame turbulization

Multiple factors are known to affect the effective flame area and thus the normal velocity of a turbulent flame. Specifically: (i) Landau–Darrieus instability, (ii) 'isothermal' flow turbulence generation in pipe flows with high Reynolds numbers, (iii) artificial flow turbulization with increasing wall roughness (e.g., that generated by Shchelkin spirals used to create varying surface roughness, (iv) the turbulence generated by the flame itself, (v) flame interaction with the near-wall boundary layer and pressure waves, resulting in finger flames, tulip flames, etc., (vi) obstacles that confine the flow and act to accelerate the flame and to interrupt the flow path, which leads to turbulence and additional flame acceleration [4,40–43]. In wide pipes, turbulence increases the flame area compared to that caused by laminar combustion, which results in flame acceleration and DDT [4]. The normal effective velocity of a turbulent flame u_+' can be determined from the sum of the normal laminar flame velocity, which is entirely determined by the physico-chemical factors [the Zel' dovich–Frank–Kamenetsky formula [3,39]] u_n, the velocity related to the 'isothermal' turbulence [generated by the flow or some turbulizers, e.g., special roughness located at the pipe wall, and all the other factors listed above [4,40–43]], v', and the velocity related to the turbulence produced by the flame itself [the third term on the right-hand side in Eq. (8)]:

$$u_+' = u_n + v' + \frac{\left(\sigma_3' - 1\right)}{\sqrt{3}} u_n \left(1 - \frac{u_n^2}{u_+'^2}\right)^{1/2} \tag{8}$$

The last two terms on the right-hand side of Eq. (8) can be approximately lumped together using the semi-empirical constant C [4]:

$$u_+' = u_n + Cv' \tag{9}$$

Turbulent pulsations in the compressed mixture behind the shock wave moving with an average velocity w are approximated as $v' = Kw$, where K is the so-called von Karman number, also a semi-empirical parameter. Accordingly, Eq. (9) yields:

$$\Delta u_+ = \frac{u_+' - u_n}{u_n} = KCw \tag{10}$$

At the beginning of a potential DDT event, the shock wave is weak, and thus $\Delta p = (p_2 - p_1)/p_1 < < 1$. Thus, Eq. (2) yields:

$$w = \frac{c_1}{\gamma}\Delta p \tag{11}$$

Combining Eqs. (10) and (11), we arrive at the following non-gasdynamics [based on Eq. (10)] relation between Δp and Δu_+:

$$\Delta p = \frac{\gamma M}{CK}\Delta u_+ \tag{12}$$

where $M = u_n/c_1$ is the Mach number based on the normal velocity of a laminar flame (a known physical parameter).

Table 1
Thermo-physical properties of several fuel-oxidizer mixtures and the corresponding values of the turbulence parameter C guaranteeing DDT at K = 0.05 in the case of ignition near the closed end of a pipe or at its center, according to Eq. (14).

Fuel-oxidizer mixture	$C_2H_2 + O_2$	$2H_2 + O_2$	$CH_4 + 2O_2$	6.3% CH_4 + 93.7% air
u_n [m/s]	10	10	3.4	0.12
q	24.2	8.96	13.8	9.35
M	3.17×10^{-2}	1.94×10^{-2}	1.02×10^{-2}	3.6×10^{-5}
qM	0.765	0.174	0.14	0.0034
C	0.42	2.74	1.70	2.98
γ	1.28	1.4	1.31	1.4

It should be emphasized that the semi-empirical approach to turbulence considered in the present section lumps the entire effect of turbulence into a single empirical parameter, the turbulence parameter C, given in Table 1. Turbulent combustion, like practically any other turbulent flow, is a highly dynamic and complex process. The reduction of such a process to a single parameter (or to 5 empirical constants as in the k-ε turbulence model, or to many more empirical constants, as in its multiple offshoots), means that an ensemble-averaged point of view is taken, while particular realizations can deviate from this approach. Specifically, DDT may or may not occur at the predicted threshold in a particular case; however, statistically, it is expected to occur, which provides a guide for engineering practice. Moreover, the lumped approach to flow description over domains $1-3$ (Fig. 1) taken in Sections 2.1 and 2.2 definitely disregards the detailed three-dimensional turbulent flow structure and would be incapable of predicting localized hot spots, resulting in triggering of DDT in domain 2, as predicted by laminar modeling of channels with exaggerated obstacles at the walls (e.g., in Refs. [13,14]). Nevertheless, turbulence provides much stronger mixing and averaging as exemplified by the velocity profile over the channel cross-section (cf. the parabolic Poiseuille velocity profile with the practically plug-one averaged turbulent velocity profile). Therefore, for a coarse estimate of DDT, one should not expect that the inaccuracy introduced by the spatial domain averaging in Sections 2.1 and 2.2 goes beyond the inaccuracy of the ensemble averaging discussed above, and the results should be understood as statistically relevant, albeit possibly missing some particular cases. Note also that the present lumped approach would be inaccurate if hot spots or strong compression zones are generated in the boundary layers near the pipe walls, as have been demonstrated in the laminar modeling of DDT in channels with obstacles [13,14]. Here, we adopt the original point of view of Shchelkin, supported by multiple experimental data on DDT in wide pipes, where the main role of the boundary layers is in generating turbulence that is rapidly transported to the flame due to the turbulent mixing and is essentially lumped in the turbulence parameter C given in Table 1.

Note also that at the beginning of a potential DDT event, deflagration also results in $\Delta p = (p_1 - p_3)/p_1 << 1$. Accordingly, for ignition near the closed end of a pipe or at its center, from Eqs. (1)–(6) (see Section 2.1), it is possible to demonstrate the following relation [4]:

$$\Delta p = \frac{qM(\Delta u_+ + 1)}{1 - qM/\gamma} \tag{13}$$

where $q = Q/(c_v T_1) = \gamma(\gamma - 1)Q/c_1^2$ is a given physical parameter of the fuel-oxidizer mixture (the dimensionless heat release in the flame), with T_1 being a given temperature of the mixture before the shock wave.

Comparison of Eqs. (12) and (13) shows that an increase in Δp results in an increase in Δu_+ and vice versa, i.e., results in DDT, if the following condition holds in the case of ignition near the closed end of a pipe [4]:

$$\frac{1}{\gamma}(qM + qCK) \geq 1 \tag{14}$$

Eq. (12) reveals that:

$$\mu = 1 + \frac{M\gamma}{CK}\left(\frac{u'_+}{u_n} - 1\right) \tag{15}$$

Once the condition set forth by Eq. (14) is satisfied, iterations are performed using Eqs. (12) and (13), revealing how DDT occurs. The pressure and velocity both increase during the iterations. Once the detonation velocity is reached, the iterations stop, at which point all of the DDT parameters in Eqs. (1)–(6) can be found.

Similarly, in the case of ignition near the open end of a pipe, the gasdynamic formula presented in Section 2.2 yields the following relation [4]:

$$\Delta p = qM^2(\Delta u_+ + 1)^2 \tag{16}$$

which replaces Eq. (13).

Accordingly, the DDT condition replacing that of Eq. (14) in this case is as follows [4]:

$$\frac{4qMCK}{\gamma} > 1 \tag{17}$$

This condition is more difficult to fulfill than that of Eq. (14), which means that it is more difficult to reach DDT when igniting a flame near an open pipe end as compared to ignition near the closed end or at the pipe center.

It should be emphasized that all the conditions for DDT (Eqs. (14) and (17)) are accompanied by the requirement that the flow behind the shock wave is turbulent, i.e., that the Reynolds number based on the pipe diameter (or its equivalent diameter) d is large enough, i.e., $Re = wd/\nu > 2300$, with ν being the molecular kinematic viscosity of the fuel-oxidizer mixture. This condition is definitely fulfilled in sufficiently large tubes.

Moreover, in relation to the DDT, the difference between a large pipe with a circular cross-section and a large tunnel (with a semi-circular cross-section) is mostly determined by the corresponding value of the semi-empirical parameter C in Eqs. (14) and (17). If the pipe and the tunnel have the same equivalent diameter, the value of C will seemingly be larger for the tunnel, which has a more complicated shape and is thus prone to generate more turbulence. Based on this simple argument (still deserving of experimental verification), the tunnel is more prone to DDT than a pipe with the same equivalent diameter.

3. Results and discussion

3.1. Transitional characteristics of DDT

The constants related to the thermo-physical properties of several fuel-oxidizer mixtures (namely, acetylene (C_2H_2)-, hydrogen (H_2)-, methane (CH_4)-oxygen, and methane (CH_4)-air mixtures) are summarized in Table 1. Note that the influence of chemistry on the flame acceleration and its role in DDT is fully lumped in the turbulence parameter C given in Table 1.

Note that the lowest value of C and the highest value of qM for the acetylene (C_2H_2)-oxygen mixture induce the most energetic DDT, according to Eq. (14). It should be emphasized that DDT may arise earlier than predicted by Eq. (14), as Eq. (14) does not account for the turbulence generated by the flame itself. Conversely, DDT may be delayed as compared to that predicted by Eq. (14), as Eq. (14) does not account for the cooling of the combustion products on the surrounding walls. The cooling effect may appear during slow acceleration of a flame in a narrow pipe. It should be emphasized that the theory presented in Section 2.3, which was used to calculate the results shown in Fig. 2, is the instability theory. Essentially, it produces time-dependent results, and thus all the parameters presented in Fig. 2 are inter-related through time, which serves as the common parameter.

The laminar flame velocity (u_n) from Table 1 was used to compute the relative flame velocity (u'_+). The relationship between Δp and Δu_+ is given by Eqs. (12) and (13), which describe the instability leading to DDT. Both Δp and Δu_+ depend on time as a common, inter-relating parameter. Fig. 2 compares the pressure ratios ($\mu = p_2/p_1$ and $\pi'_3 = p_3/p_1$) and the density ratio ($\sigma'_3 = \rho_1/\rho_3$) predicted for DDT in the acetylene (C_2H_2)-, hydrogen (H_2)-, and methane (CH_4)-oxygen mixtures, and in the methane (CH_4)-air mixture case. Both μ and π'_3 increased as u'_+ increased for all cases. The value of μ was much greater than that of π'_3, indicating that p_2, the pressure of the compressed gas between the shock wave and the flame front, is significantly higher than the pressure of the combustion products. This shows, as expected, that the flame is essentially a rarefaction wave due to the combustion reaction heat released in it. The increase in μ (or p_2) was most prominent in the case of the acetylene-oxygen mixture, a shown in Fig. 2(a). On the other hand, the increase in μ was the smallest for the methane-air mixture (Fig. 2(d)) due to interference from species other than oxygen in the air. This makes it clear that the DDT phenomenon depends strongly on the oxidizer type. The corresponding density ratio decreased (σ'_3) as u'_+ increased, which indicates that the density of the combustion products (ρ_3) increased, while approaching the maximum detonation velocity (D_{max}); note that the detonation velocity D is described by:

$$D/c_1 = \{[(\gamma+1)\mu + (\gamma-1)]/2\gamma\}^{1/2} \tag{18}$$

Notably, the value of $\sigma_3{}'$ approaches unity, whereas the detonation velocity reached D_{max}, which indicates that the density of the combustion products (ρ_3) became equal to the density of the mixture before the shock wave (ρ_1) near the end of the transition.

Fig. 2 shows that the velocities D, U, and w increased for all cases subsequent to the increase in u'_+. Hydrogen has the highest velocities of detonation, flame, and compressed mixture behind the shock wave (D, U, and w, respectively). The methane-air mixture (Fig. 2(d)) gives rise to the lowest velocities because of the relative lack of oxygen during combustion. The flame velocity is defined by $U = u'_+ + w$, and thus U is always higher than w. Initially, the flame velocity U is equal to the velocity of the compressed mixture gas behind the shock wave, w. However, as u'_+ increases, U also increases, and eventually the flame velocity U reaches the detonation velocity, D. All these computations were stopped when the maximum detonation velocity D_{max} was reached, corresponding to $D_{max} = 2363$, 2800, 2320, and 1650 ms^{-1} for Fig. 2(a)–(d), respectively [4,43].

It should be emphasized that the present theory relates the deflagration-to-detonation transition to the flame instability and turbulization. The upper limit of the characteristic time of this process is $t \sim d/(2\pi u_n)$ where d is the pipe diameter [3]. Accordingly, the evolution of all the parameters presented in Figs. 2 corresponds to this time interval. Taking for the estimate $d = 5$ cm and $u_n = 10$ m/s, one finds $t \sim 1$ ms, and with $D \sim 2500$ m/s, the transition length would be on the scale of 2.5 m, i.e. 50 pipe diameters, which is a plausible estimate of the upper limit [3].

3.2. Comparison with experimental data

Fig. 3 presents a comparison of the theoretical predictions of the pressure (p_2) rise with the experimental data for several methane and hydrogen concentrations in the mixtures for the steady-state case. Notably, the newly developed model is

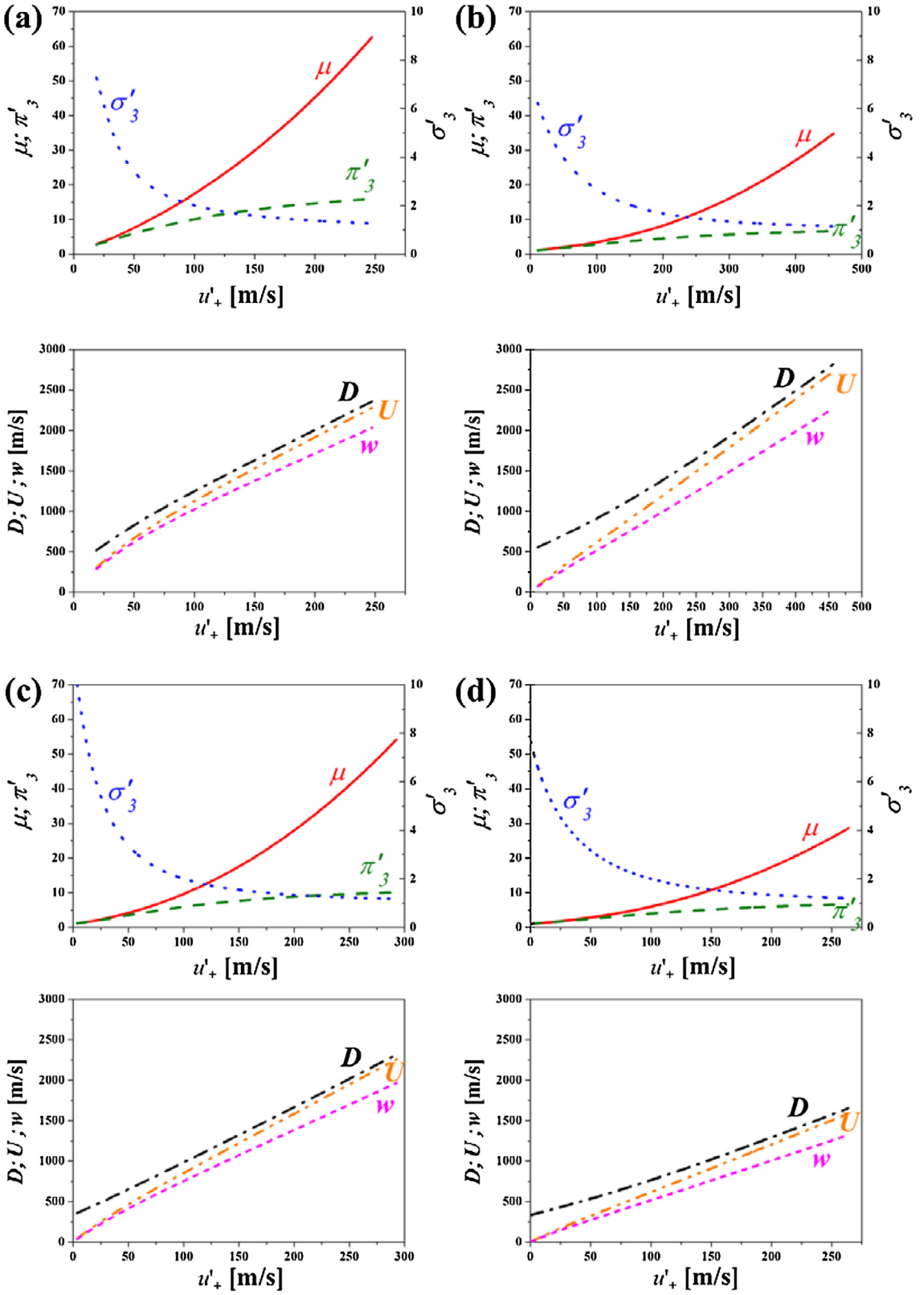

Fig. 2. DDT characteristics for cases with: (a) acetylene (C_2H_2)-, (b) hydrogen (H_2)-, (c) methane (CH_4)-oxygen mixture, and (d) methane (CH_4)-air mixture.

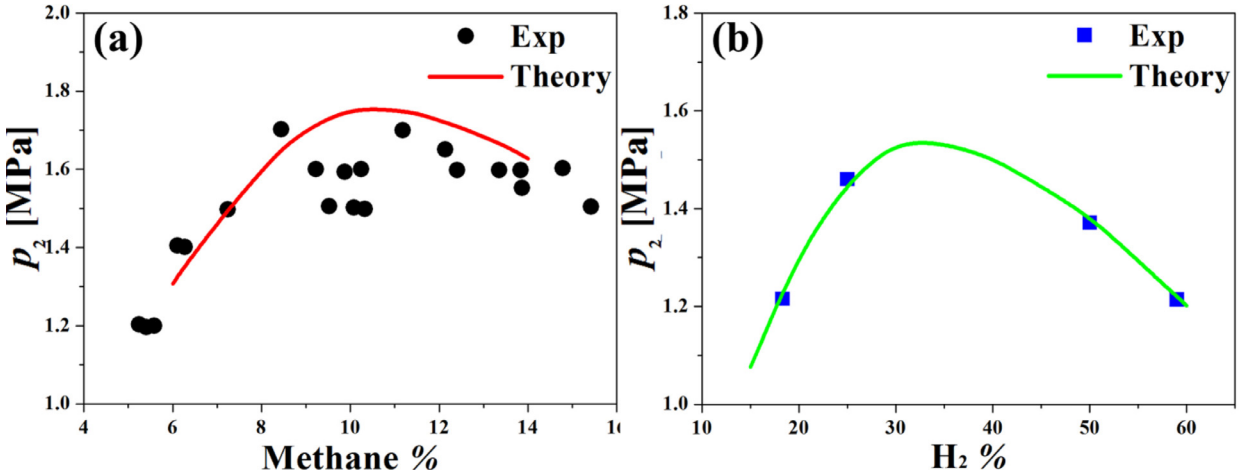

Fig. 3. Comparison of pressure (p_2) rise from experimental data in Refs. [43,44] with theoretical predictions for: (a) methane and (b) hydrogen combustion. Note that p_2 is the compressed gas pressure between the shock wave and flame front in domain 2.

capable of predicting the transition, as demonstrated in Fig. 2, whereas the theory implemented in Refs. [43,44] is capable of predicting the steady-state case only. For the theoretical predictions in Fig. 3(a), the experimental values of the laminar flame velocity, detonation velocity, and detonation pressure from Refs. [43,45] were used. The experimental data for the pressure rise in Ref. [43] was reported to have an error margin of about ± 0.3 MPa because of the possibility of an igniter problem during the experiment near the stoichiometric ratio. Nevertheless, the agreement between the predictions and the data in Fig. 3(a) appears to be reasonable, albeit with minor distinctions attributed to the heat loss associated with radiation from soot.

For the hydrogen-containing mixtures (Fig. 3(b)), the experimental values of the laminar flame velocity, detonation velocity, and detonation pressure p_2 were adopted from Refs. [44,46,47]. The comparison of the predictions with the data is quite accurate in this case, which implies that the absence of soot during hydrogen combustion minimized the uncertainty level in the experimental measurements.

It should be emphasized that the experiments presented in Ref. [43] with detonation initiation in the pipes revealed detonation waves propagating close to the limiting sonic Chapman–Jouguet regime. The present predictions of the pressure (p_2) rise depicted in Fig. 3 agree with this set of data, and thus essentially point at instability, leading to the Chapman–Jouguet regime. Note, that this is the upper limit, and under certain conditions, the experiments and numerical simulations revealed initiation of the detonation waves before this condition is fulfilled. Specifically, detonation waves can also be preliminary initiated in three-dimensional pockets between the shock and deflagration waves that result from non-uniformity, extreme turbulence with localized high-pressure zones, etc. (i.e., essentially by the thermal explosion mechanism responsible for knocking in spark ignition engines) [48]. In such cases, the present analytical theory would be inapplicable and a detailed numerical investigation is required.

3.3. Prediction of DDT

Fig. 4 shows the experimental images of the DDT phenomenon during hydrogen combustion inside a compartment that was initially filled with 22.5% hydrogen and 77.5% air in our previous experiments [49]. According to our previous experiment [49], the measurement was quite reliable with an uncertainty level of less than 8%. The same p_{max} and nearly the same impulses and effective duration within the variation of 8% were ensured. The pressure (100 kHz), a high speed video (3000 frames per second, fps), and a high definition (HD) video (30 fps) were recorded for this test. A total of seventeen dynamic pressure gauges captured the pressure history within and outside the experimental apparatus. These images were acquired with a high-speed camera at a frame rate of 3000 fps. Fig. 4(a) and (b) present the time series snapshots with an interval of 0.7 ms. The dimensions of the compartment were $7.3 \times 14.6 \times 3.7\ m^3$. About two-hundred cylindrical pipes with diameters of 5 cm were regularly aligned inside the compartment, corresponding to the congested-space scenario. These columnar pipes are visible behind the white plastic ruptured sheet in Fig. 4. When the hydrogen gas inside the compartment was ignited, blasting waves and flames were unleashed, which ruptured the white plastic sheet covering the front of the compartment. During the flame blasting, the congested-space with the pipes in the compartment promoted local turbulization and caused sporadic DDT phenomena, resulting in subsequent pressure build-up; Fig. 5 illustrates this phenomenon. It should be emphasized that this experiment is quite different from that illustrated in Fig. 1, which considered a gas-filled tube in which blasting waves propagate. On the other hand, in the experiment depicted in Fig. 4, the entire compartment was filled with hydrogen gas, i.e., the entire compartment played the role of the pipe of Fig. 1. At the same time, the vertical pipelines were purposely installed to create congested conditions, which facilitated turbulization. The seminal work of Shchelkin demonstrated that even tiny obstacles installed inside a pipe of the type shown in Fig.

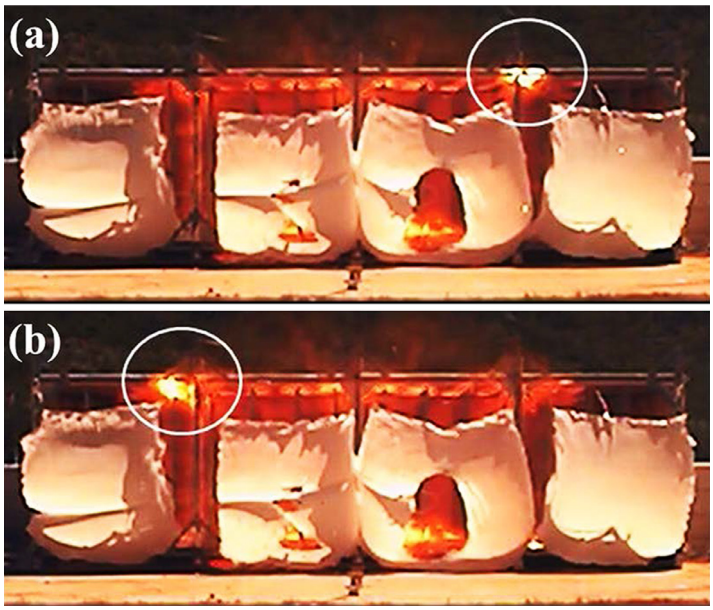

Fig. 4. Locally observed (the circled areas) DDT phenomenon during hydrogen combustion inside a compartment that was initially sealed with white plastic covers, which were detached after combustion. The hydrogen concentration was 22.5% and the air concentration was 77.5%. Note that the compartment was filled with cylindrical pipelines, leading to congestion. Both left and right ends of the compartment, as well as the back-side, are unyielding closed walls. Ignition was initiated by a spark from the back wall. The high-speed CCD camera was operated at 3000 frames per second. The velocity of the pressure wave was estimated to be around 1700 m/s.

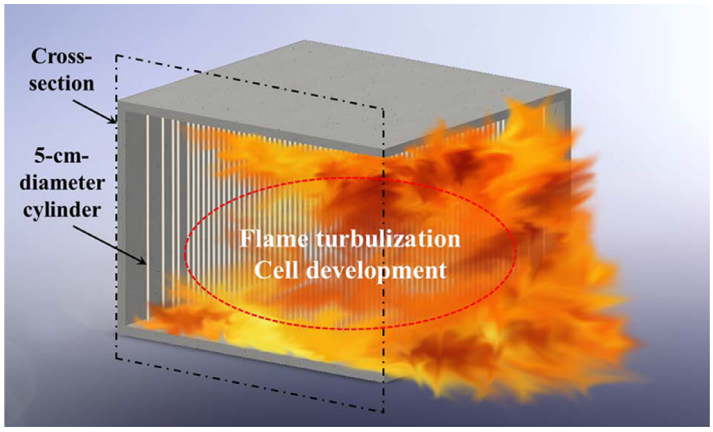

Fig. 5. Flame turbulization induced by obstacles in a congested area.

1 greatly facilitate turbulization of the gas flow, and thus, the DDT. The same role, to an even greater extent, is played by the obstacle pipes inserted in the compartment in Fig. 4. In particular, in some local areas encircled in Fig. 4, detonation was observed due to enhanced turbulization arising from the designed congestion with numerous vertical pipelines. Namely, the two images in Fig. 4 were acquired almost simultaneously. The hot spots are marked with circles at the top boundary of the compartment. These hot spots were further investigated with locally installed pressure sensors at a regular interspace distance. The locations of the pressure sensors are described in our previous report [49].

When the pressure rise was detected at a sensor, the second closest sensor also measured a similar pressure rise at a measurable time delay. Because the inter-sensor distance was known and the time between the first and second detection was known, the velocity of the pressure wave could be estimated, i.e., about $\sim$ 1700 ms^{-1} for both images in Fig. 4(a) and (b).

The DDT was explored using a fuel-oxidizer mixture comprising 22.5% H_2 and 77.5% air. The flame velocity used for the predictions was 1700 ms^{-1}, as in the experiment. The value of the coefficient C was 3. The pressure rise during the experiment was measured to be about 0.7 MPa, whereas the theoretically predicted p_3 was found to be about 0.74 MPa with a laminar flame velocity of 1.1 ms^{-1} [46,50]. Thus, the agreement is quite close. Note that p_3 is the pressure of the combustion products in domain 3 in Fig. 1.

4. Conclusion

The analytical DDT theory was shown to accurately predict the pressure rise and the shock wave speed, being congruent with the empirical data. The developed theory predicts the transitional characteristics of DDT, which may develop during ignition of flammable gas leaks in a petrochemical power plant. Hazard and Operability Review (HAZOP) is required for the safety design of petrochemical plants, for which prediction of the overpressure using the developed theory can provide an accurate estimation for hypothetical accident scenarios. Both the theory and experiments showed the highest value of the compressed gas pressure to be around $p_2 = 1.7$ MPa for methane and hydrogen. The theory was also capable of predicting the pressure of the combustion products behind the deflagration front for hydrogen combustion ($p_3 \sim 0.7$ MPa) with sufficient congruence with the experimentally measured value. This predictive capability of the DDT theory should be of practical interest to field-safety engineers for the design and assessment of petrochemical plants.

Acknowledgement

This work was supported by the National Research Council of Science & Technology (NST) grant by the Korea government (MSIP) (No. CRC-16-02-KICT). This research was supported by the Technology Development Program to Solve Climate Changes of the National Research Foundation (NRF) funded by the Ministry of Science, ICT & Future Planning (NRF-2016M1A2A2936760, NRF-2013R1A5A1073861, and NRF-2017R1A2B4005639).

References

[1] R. Courant, K.O. Friedrichs, Supersonic Flow and Shock Waves, Springer, Heidelberg, 1976.
[2] L.D. Landau, E.M. Lifshitz, Fluid Dynamics, Pergamon Press, Oxford, 1987.
[3] Y.B. Zel'dovich, G.I. Barenblatt, V.B. Librovich, G.M. Mahviladze, Mathematical Theory of Combustion and Explosions, Plenum Press, New York, 1985.
[4] K.I. Shchelkin, Y.K. Troshin, Gasdynamics of Combustion, Mono Book Corporation, Baltimore, 1965.
[5] J.H.S. Lee, Dynamic parameters of gaseous detonations, Ann. Rev. Fluid Mech. 16 (1984) 311–336.
[6] A.K. Oppenheim, R.I. Soloukhin, Experiments in gasdynamics of explosions, Ann. Rev. Fluid Mech. 5 (1973) 31–58.
[7] D. Valiev, in: Licentiate Thesis, Royal Institute of Technology, Stockholm, 2007.
[8] P.A. Urtiew, A.K. Oppenheim, Experimental observations of the transition to detonation in an explosive gas, Proc. R. Soc. Lond. A Math. Phys. Eng. Sci. 295 (1966) 13–28.
[9] H. Matsui, Detonation propagation limits in homogeneous and heterogeneous systems, Journal de Physique IV (Proceedings), EDP Sciences 12 (2002) 11–17.
[10] W. Bartknecht, Explosions: Course, Prevention, Protection, Springer Verlag, Berlin, 1981.
[11] M. Gerstein, E.R. Carlson, F.U. Hill, Natural gas-air explosions at reduced pressure, Ind. Eng. Chem. 46 (1954) 2558–2562.
[12] Y.B. Zeldovich, V.B. Librovich, G.M. Makhviladze, G.I. Sivashinsky, On the development of detonation in a non-uniformly preheated gas, Astronaut. Acta 15 (1970) 313–321.
[13] V.N. Gamezo, T. Ogawa, E.S. Oran, Flame acceleration and DDT in channels with obstacles: effect of obstacle spacing, Combust. Flame 155 (2008) 302–315.
[14] V.N. Gamezo, T. Ogawa, E.S. Oran, Numerical simulations of flame propagation and DDT in obstructed channels filled with hydrogen–air mixture, Proc. Combust. Inst. 31 (2007) 2463–2471.
[15] G.B. Goodwin, R.W. Houim, E.S. Oran, Shock transition to detonation in channels with obstacles, Proc. Combust. Inst. 36 (2017) 2717–2724.
[16] T. Ogawa, V.N. Gamezo, E.S. Oran, Flame acceleration and transition to detonation in an array of square obstacles, J. Loss Prev. Process Ind. 26 (2013) 355–362.
[17] D. Valiev, V. Bychkov, V. Akkerman, L.-E. Eriksson, M. Marklund, Heating of the fuel mixture due to viscous stress ahead of accelerating flames in deflagration-to-detonation transition, Phys. Lett. A 372 (2008) 4850–4857.
[18] D. Valiev, V. Bychkov, V. Akkerman, C.K. Law, L.-E. Eriksson, Flame acceleration in channels with obstacles in the deflagration-to-detonation transition, Combust. Flame 157 (2010) 1012–1021.
[19] D. Valiev, V. Akkerman, M. Kuznetsov, L.-E. Eriksson, C.K. Law, V. Bychkov, Influence of gas compression on flame acceleration in the early stage of burning in tubes, Combust. Flame 160 (2013) 97–111.
[20] V. Bychkov, V.y. Akkerman, G. Fru, A. Petchenko, L.-E. Eriksson, Flame acceleration in the early stages of burning in tubes, Combust. Flame 150 (2007) 263–276.
[21] C. Clanet, G. Searby, On the "tulip flame" phenomenon, Combust. flame 105 (1996) 225–238.
[22] H. Xiao, R.W. Houim, E.S. Oran, Effects of pressure waves on the stability of flames propagating in tubes, Proc. Combust. Inst. 36 (2017) 1577–1583.
[23] L. Kagan, G. Sivashinsky, Parametric transition from deflagration to detonation: Runaway of fast flames, Proc. Combust. Inst. 36 (2017) 2709–2715.
[24] I. Brailovsky, G. Sivashinsky, Hydraulic resistance as a mechanism for deflagration-to-detonation transition, Combust. Flame 122 (2000) 492–499.
[25] L. Kagan, G. Sivashinsky, Autoignition due to hydraulic resistance and deflagration-to-detonation transition, Combust. Flame 154 (2008) 186–190.
[26] M.A. Liberman, M.F. Ivanov, A.D. Kiverin, M.S. Kuznetsov, A.A. Chukalovsky, T.V. Rakhimova, Deflagration-to-detonation transition in highly reactive combustible mixtures, Acta Astronaut. 67 (2010) 688–701.
[27] M.F. Ivanov, A.D. Kiverin, I.S. Yakovenko, M.A. Liberman, Hydrogen–oxygen flame acceleration and deflagration-to-detonation transition in three-dimensional rectangular channels with no-slip walls, Int. J. Hydrogen Energy 38 (2013) 16427–16440.
[28] M.A. Liberman, M. Kuznetsov, A. Ivanov, I. Matsukov, Formation of the preheated zone ahead of a propagating flame and the mechanism underlying the deflagration-to-detonation transition, Phys. Lett. A 373 (2009) 501–510.
[29] M.F. Ivanov, A.D. Kiverin, M.A. Liberman, Flame acceleration and DDT of hydrogen–oxygen gaseous mixtures in channels with no-slip walls, Int. J. Hydrogen Energy 36 (2011) 7714–7727.
[30] M.A. Liberman, A.D. Kiverin, M.F. Ivanov, On detonation initiation by a temperature gradient for a detailed chemical reaction models, Phys. Lett. A 375 (2011) 1803–1808.
[31] M.F. Ivanov, A.D. Kiverin, M.A. Liberman, Ignition of deflagration and detonation ahead of the flame due to radiative preheating of suspended micro particles, Combust. Flame 162 (2015) 3612–3621.
[32] M.A. Liberman, M.F. Ivanov, A.D. Kiverin, Effects of thermal radiation heat transfer on flame acceleration and transition to detonation in particle-cloud hydrogen flames, J. Loss Prev. Process Ind. 38 (2015) 176–186.
[33] M.A. Liberman, M.F. Ivanov, A.D. Kiverin, Radiation heat transfer in particle-laden gaseous flame: flame acceleration and triggering detonation, Acta Astronaut. 115 (2015) 82–93.
[34] A.Y. Poludnenko, T.A. Gardiner, E.S. Oran, Spontaneous transition of turbulent flames to detonations in unconfined media, Phys. Rev. Lett. 107 (2011) 054501.

[35] L. Kagan, G. Sivashinsky, The transition from deflagration to detonation in thin channels, Combust. Flame 134 (2003) 389–397.
[36] G. Ciccarelli, S. Dorofeev, Flame acceleration and transition to detonation in ducts, Prog. Energy. Combust. Sci. 34 (2008) 499–550.
[37] B. Bang, H. Park, J. Kim, S.S. Al-Deyab, A.L. Yarin, S.S. Yoon, Simplified method for estimating the effect of a hydrogen explosion on a nearby pipeline, J. Loss Prev. Process Ind. 40 (2016) 112–116.
[38] B. Bang, H. Park, J. Kim, S.S. Al-Deyab, A.L. Yarin, S.S. Yoon, Analytical and numerical assessments of local overpressure from hydrogen gas explosions in petrochemical plants, Fire Mater. 41 (2017) 587–597.
[39] D.A. Frank-Kamenetsky, Diffusion and Heat Transfer in Chemical Kinetics, Plenum Press, New York, 1969.
[40] B.E. Gelfand, M.V. Silnikov, S.P. Medvedev, S.V. Khomik, Thermo-Gas Dynamics of Hydrogen Combustion and Explosion, Springer, Heidelberg, 2012.
[41] H. Xiao, R.W. Houim, E.S. Oran, Formation and evolution of distorted tulip flames, Combust. Flame 162 (2015) 4084–4101.
[42] H. Xiao, X. Shen, S. Guo, J. Sun, An experimental study of distorted tulip flame formation in a closed duct, Combust. Flame 160 (2013) 1725–1728.
[43] R.K. Zipf Jr, V.N. Gamezo, M.J. Sapko, W.P. Marchewka, K.M. Mohamed, E.S. Oran, D.A. Kessler, E.S. Weiss, J.D. Addis, F.A. Karnack, Methane–air detonation experiments at NIOSH lake Lynn laboratory, J. Loss Prev. Process Ind. 26 (2013) 295–301.
[44] P.M. Ordin, Safety Standard for Hydrogen and Hydrogen Systems: Guidelines for Hydrogen System Design, Materials Selection, Operations, Storage, and Transportation. Office of Safety and Mission Assurance, National Aeronautics and Space Administration, Washington DC, 1997.
[45] G.E. Andrews, D. Bradley, The burning velocity of methane-air mixtures, Combust. Flame 19 (1972) 275–288.
[46] A.E. Dahoe, Laminar burning velocities of hydrogen–air mixtures from closed vessel gas explosions, J. Loss Prev. Process Ind. 18 (2005) 152–166.
[47] T. Ginsberg, G. Ciccarelli, J. Boccio, Initial Hydrogen Detonation Data From The High-Temperature Combustion Facility, Brookhaven National Laboratory, Upton, NY, USA, 1994.
[48] E. Moses, A.L. Yarin, P. Bar-Yoseph, On knocking prediction in spark ignition engines, Combust. Flame 101 (1995) 239–261.
[49] B.-H. Bang, C.-S. Ahn, J.-G. Lee, Y.-T. Kim, M.-H. Lee, B. Horn, D. Malik, K. Thomas, S.C. James, A.L. Yarin, Theoretical, numerical, and experimental investigation of pressure rise due to deflagration in confined spaces, Int. J. Therm. Sci. 120 (2017) 469–480.
[50] R.D. McCarty, J. Hord, H.M. Roder, Selected properties of hydrogen (engineering design data), National Engineering Lab, Boulder, CO, USA, 1981.